

II.2

FLOATING ZONE STABILITY (EXP. 1-ES-331)

I. Da Riva I. Martínez

Polytech. Univ. of Madrid, Spain

The present state of the preparation of an experiment on floating liquid zones to be performed in the first Spacelab flight is presented. In this experiment, a liquid bridge is to be placed between two parallel coaxial disks (in the Fluid Physics Module) and subjected to very precise disturbances in order to check the theoretical predictions about its stability limits and behavior under mechanical inputs: stretching of the zone, filling or removing the liquid, axial vibration, rotation, disalignment, etc. Several aspects of the research are introduced: 1) Relevance of the study. 2) Theoretical predictions of the liquid behavior regarding the floating-zone stability limits and the expected response to vibrational and rotational disturbances. 3) Ground support experiments using the Plateau technique or the small scale simulation. 4) Instrumental aspects of the experimentation: the Fluid Physics Module utilization and post-flight data analysis. 5) Research program for future flights.

Keywords: Floating Zone, Spacelab Experiments, Capillary Instability, Spin-up.

1. RELEVANCE

An intermediate approach to the setting-up of Materials-Science experiments in Space is the floating-zone technique. It combines some of the advantages of cartridges (where the sample is totally enclosed and surface effects are hidden) and those of the containerless management (where drops are kept floating isolated and surface effects are dominant, offering the unique performances of an easy control of positioning and disturbances to be applied. Because of these interesting features, with the advent of space labs, floating zones have deserved a major attention; the first demonstration was made onboard Skylab IV (Ref. 1), and Spacelab 1 promises to boost their knowledge.

The importance of the floating zone technique in crystal growth, both on ground and in space, is well known (Ref. 2), and many applications require (or would greatly benefit from) it: among them, those based on surface chemistry (wetting (Ref. 3), spreading (Ref. 4), coalescence, adsorption, etc.), other surface phenomena such as Marangoni convection (Ref. 5), and so on. Aside from the valuable contribution to the new field of microgravitational fluidmechanics, the aim of the proposed research is to provide some sound assessment to the users of the floating-zone technique.

2. THEORETICAL PREDICTIONS

The idealized floating zone is a mass of liquid held by interfacial forces between two parallel coaxial disks, as Fig. 1 sketches.

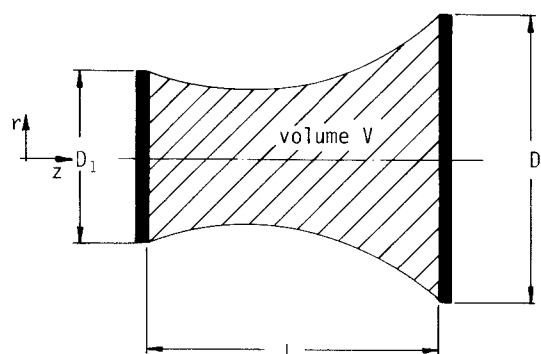


Figure 1. Sketch of a floating zone.

a 30 minutes animated-motion film has been produced that gives a good idea of the expected behavior of floating zones.

2.1 Equilibrium shapes

Assuming the liquid anchored at the disk edges (what seems to be the most likely under normal circumstances) Laplace theory of surface tension provides a simple formulation of the problem of determining the equilibrium shape that a volume V of liquid will adopt when placed between two parallel coaxial disks of diameter D_1 and D_2 respectively, standing a distance L apart. The statement of the problem can be as follows:

Let $r(z)$ be the surface of revolution separating the liquid from its environment; equilibrium requires uniform temperature all through and uniform pressure in closed domains; at the interface, surface tension causes the pressure having a jump proportional to the curvature. Thence, $r(z)$ is a constant-curvature surface of revolution to be found from

$$\frac{r''}{(1+r'^2)^{3/2}} - \frac{1}{r(1+r'^2)^{1/2}} = \text{cte} = p_{\text{ext}} - p_{\text{int}} \quad (1)$$

subject to the conditions

$$r(z=z_1) = D_1/2 \tag{2}$$

$$r(z=z_2) = D_2/2 \tag{3}$$

$$\pi \int_{z_1}^{z_2} r^2 dz = V \tag{4}$$

$$z_2 - z_1 = L \tag{5}$$

Scaling with D_1 for instance, the solution only depends on three nondimensional parameters: $D_2/D_1 = a$, $L/D_1 = l$ and $V/D_1^3 = v$, and can be analytically obtained (although in an implicit parametric form): Table 1 sums up the found solution with some useful related functions, namely, the area of the free surface and the pressure jump across it.

2.2 Stability

The parametric solution just presented is not suitable for direct computation of $r(z)$ for a given set (a, l, v) , and solving numerically the two-points-boundary-value problem (Eqs. 1 to 5) is still simpler, in spite of the iterative process implied. Nevertheless, this parametric solution is very useful because it allows for a direct evaluation of its stability without having to apply the standard variational criteria (Jacobi equation) or even going to dynamic stability studies. In fact, as a consequence of the smoothly dependence of the shape with respect to the chosen parameters, the loss of stability will take place in a point where multiplicity occur in its neighborhood, that is, when the Jacobian of the transformation vanishes:

$$\frac{\partial(a, l, v)}{\partial(\alpha, \phi_1, \phi_2)} = J(\alpha, \phi_1, \phi_2) \tag{6}$$

This equation defines a surface separating the region of stability from that of instability; in the case $a = 1$ (equal disks) it reduces to the lower bounding curve in Fig. 2 and represents the minimum volume of liquid required to bridge the disks (as a function of the slenderness: disk separation / disk diameter ratio).

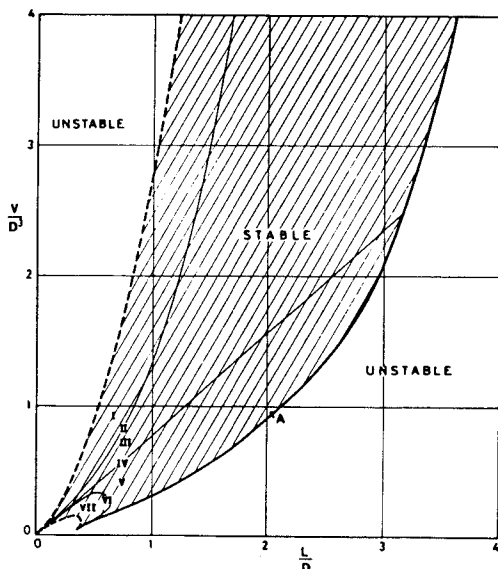


Figure 2. Stability limits of a floating zone. II: spherical zones; IV: cylindrical zones; VI: catenoidal zones.

2.3 Nearly cylindrical zones

The circular cylinder is a shape of constant curvature, thus, a possible solution of the problem stated in § 2.1 (indeed the most obvious one). It also happens that cylindrical zones are the most widely used, either because of its simpler geometry (that makes its analysis easier), or because of the application itself (as in the purification of rod-shaped semiconductor materials, sketched in Fig. 3).

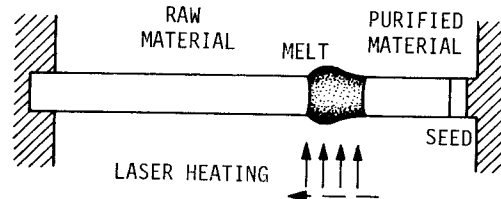


Figure 3. Purification of materials by means of the floating-zone technique.

Therefore, it is worthwhile looking to deviations from the perfect cylindrical shape caused by either an excess of liquid volume (representing perhaps the dilatation shown in Fig. 3) or a residual gravity or inertial force field; results from both problems are plotted in Figs. 4 and 5, respectively.

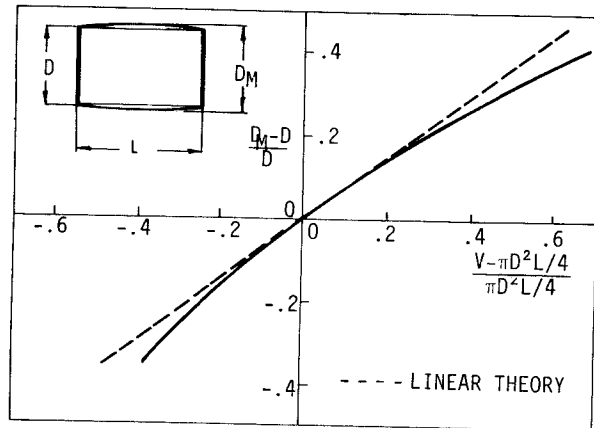


Figure 4. Maximum deviation from a cylindrical shape due to a liquid excess. $L/D = 2$.

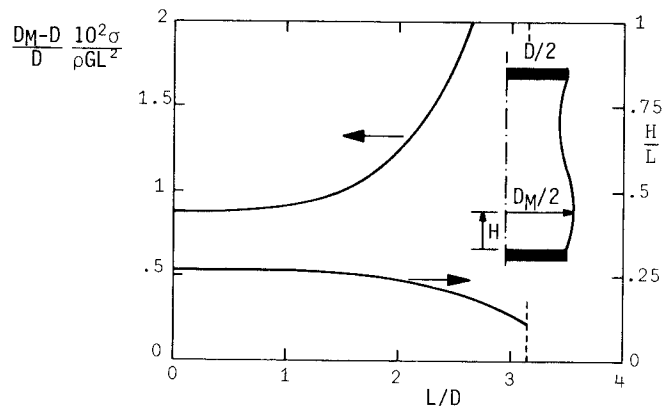


Figure 5. Maximum deviation from a cylindrical shape due to a small axial gravity. Lateral gravity causes a bend with maximum deflection $r_M = D/2 = \rho G L^2 D / (16 \sigma)$, G being the acceleration and σ the surface tension.

Table 1. Parametric solution for the equilibrium shapes of a floating liquid zone at rest.

$$l(\phi_1, \phi_2, \alpha) = \frac{L}{D_1} = \frac{1}{2} \frac{B(\phi_2, \alpha) - B(\phi_1, \alpha)}{A(\phi_1, \alpha)}$$

$$v(\phi_1, \phi_2, \alpha) = \frac{V}{D_1^3} = \frac{1}{2} \frac{C(\phi_2, \alpha) - C(\phi_1, \alpha)}{A^3(\phi_1, \alpha)}$$

$$a(\phi_1, \phi_2, \alpha) = \frac{D_2}{D_1} = \frac{A(\phi_2, \alpha)}{A(\phi_1, \alpha)}$$

$$r(\phi, \phi_1, \phi_2, \alpha) = \frac{1}{2} \frac{A(\phi, \alpha)}{A(\phi_1, \alpha)}$$

$$z(\phi, \phi_1, \phi_2, \alpha) = \frac{1}{2} \frac{B(\phi, \alpha)}{A(\phi_1, \alpha)}$$

$$s(\phi_1, \phi_2, \alpha) = \frac{1}{2} \frac{D(\phi_2, \alpha) - D(\phi_1, \alpha)}{A^3(\phi_1, \alpha)} \quad (\text{free surface area})$$

$$p(\phi_1, \phi_2, \alpha) = \frac{4 A(\phi_1, \alpha)}{1 + \cos \alpha} \quad (\text{pressure jump})$$

Functions A, B, C, and D are defined as follows:

$$A(\phi, \alpha) = (1 - \sin^2 \alpha \sin^2 \phi)^{1/2}$$

$$B(\phi, \alpha) = \cos \alpha F(\phi, \alpha) + E(\phi, \alpha)$$

$$C(\phi, \alpha) = \pi \{ \sin^2 \alpha \sin \phi \cos \phi A(\phi, \alpha) - \cos \alpha B(\phi, \alpha) + 2(1 + \cos \alpha)^2 E(\phi, \alpha) \} / 12$$

$$D(\phi, \alpha) = \pi(1 + \cos \alpha) E(\phi, \alpha)$$

where F and E state for the elliptic integrals of first and second class (their series expansion is recommended for numerical computation, following the iterative process:

$$\begin{aligned} F_0 &= \phi & F_n &= F_{n-1} + J_n I_n \sin^{2n} \alpha \\ E_0 &= \phi & E_n &= E_{n-1} - K_n I_n \sin^{2n} \alpha \\ I_0 &= \phi & I_n &= I_{n-1} \left(1 - \frac{1}{2n}\right) - \frac{\cos \phi}{2n} \sin^{2n-1} \alpha \\ J_0 &= 1 & J_n &= J_{n-1} \left(1 - \frac{1}{2n}\right) \\ K_0 &= -1 & K_n &= K_{n-1} \left(1 - \frac{3}{2n}\right) \end{aligned}$$

to be stopped when the required accuracy is attained).

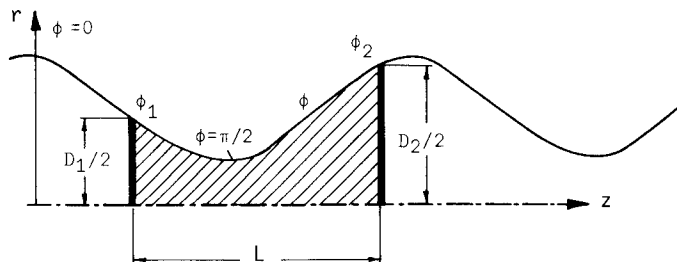
The range of the four parameters involved in the parametric solution are (see sketch):

$$0 \leq \alpha \leq \pi \quad \left\{ \alpha = \arccos \frac{r(\phi=\pi/2)}{r(\phi=0)} \right\}$$

$$0 \leq \phi_1 \leq \pi$$

$$\phi_1 \leq \phi_2 \leq \phi_1 + \pi$$

$$\phi_1 \leq \phi \leq \phi_2$$



2.4 Effect of axially spinning a cylindrical zone

The cylindrical shape is the only equilibrium solution not altered by the presence of a centrifugal force field, which only affects the pressure field inside the zone.

Notwithstanding the fact that the shape is preserved, the effect of rotation upon its stability is of paramount importance: first, because the stability range is reduced, and second, because a new breakage mode appears, leading the liquid spun out of the zone; Figure 6 presents the different unstable modes and their respective limits.

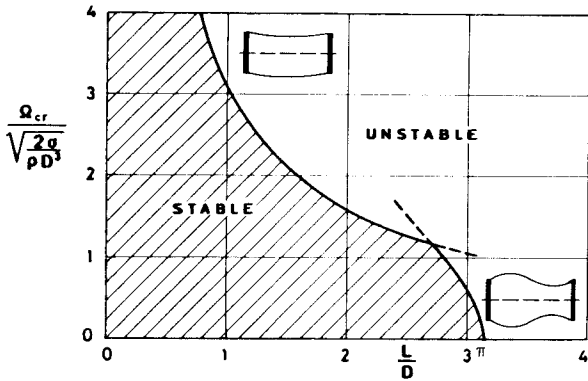


Figure 6. Critical angular speed for an axially spinning cylindrical zone.

2.5 Effect of an axial vibration on a cylindrical zone

If floating zones are to be used in space laboratories, surrounded by working equipment, and the crew moving around, it is obvious that the floating-zone end-disks will always be subjected to oscillations, and a careful analysis of its consequences (outer shape deformation, reduced stability, internal currents, etc.) is badly needed from the beginning.

Assuming an inviscid liquid forming a cylindrical zone between two disks mounted on a vibrating frame, linear theory predicts a reduction of the stability limit ($L/D = \pi$ without rotation) as plotted in Fig. 7. The influence of the forcing frequency is so marked that for values smaller than the critical one the zone is hardly disturbed.

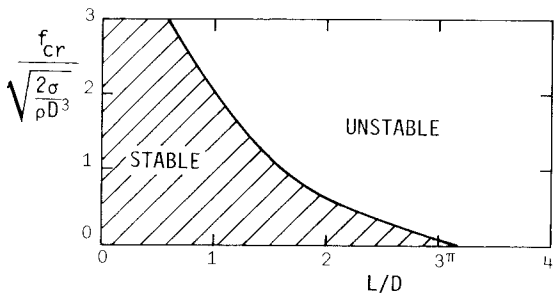


Figure 7. Critical frequency for an axially vibrating cylindrical zone.

In the experimental set-up (Fluid Physics Module) intentional vibrations are to be introduced only through one of the disks, hence a volume oscillation (relatively to the cylinder) will be present.

2.6 Spin-up of a floating liquid zone

Spin-up problems have deserved a major attention since Kármán's pioneering work (Ref. 6), giving rise to a widespread utilization in physicochemical hydrodynamics; a fairly recent review can be found in Ref. 7. The centrifugal flux that all these models predict is not compatible with the obvious assumption of the free surface remaining anchored at the disk edge, but under certain circumstances (disks not too close, low viscosity liquid) the problem can be decoupled in several regions where the effects are concentrated and matched-asymptotic-expansion methods applied. In that case, the disks do not interfere with each other (at least for small times), the central region is not influenced by the free surface, and the only new feature is the appearance of a corner region where the spun-up outflow adapts to the impenetrability condition at the free surface, attached to the disk edge. The most relevant results of the work performed is that the free surface do not slope in the immediate vicinity of the disk, as Fig. 8 sketches.

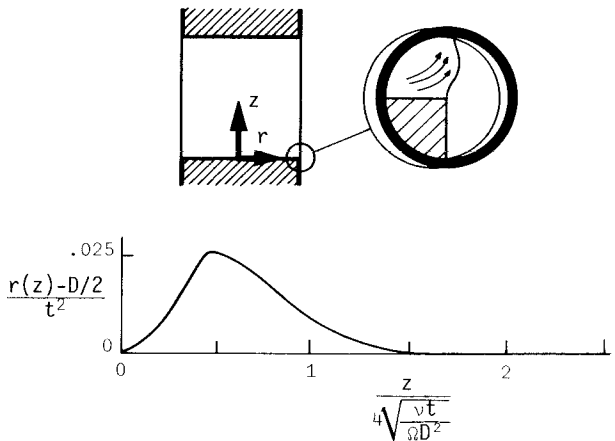


Figure 8. a) Sketch of the corner region. b) Deflection of the free surface near the disk, for small times after start of rotation.

3. GROUND SUPPORT EXPERIMENTS

Interfacial forces are bound to play a significant part on ground only if the characteristic length is very small, due to the preponderance of hydrostatic pressure; in fact, it is to overcome this constrain why one goes to orbiting laboratories. In spite of that, some useful terrestrial work can be performed by suitable simulation arrangements, as soap films, neutral buoyancy baths (Plateau's tank), small scale experimentation, or using a levitating force (hydrodynamical, acoustical, electromagnetic, etc.).

The drawbacks of all these weightlessness simulations are such that only a merely qualitative insight can be gained, but they are of great help for the preparation of the flight equipment (for handling, visualizing and recording). Consequently, we have set up several test rigs: a soap-film column-maker, a Plateau tank with vibrational and rotational capabilities, and a spinning table specially designed to deal with flat floating-zones (250 mm ϕ , 5 mm height) for assessment on the crucial aspect of the liquid liquid behavior near the disk edge (the thymol-blue technique of local color change by a pH indicator is used to visualize the flow pattern). In addition to that, we are considering the possibility of setting up a microzone facility.

4. INSTRUMENTAL ASPECTS

Experimentation is thought as an iterative process directly performed by the investigator; unfortunately, the huge costs of space research have forced it to change to a "one stroke" trial carried out by a very busy astronaut operating a mazy multiuser facility. The best way to cope with this handicap is by having a Ground Support Facility where investigators, operators and instruments could have the required iterative interaction (testing the equipment for feasibility, development and improvement analysis, training the payload specialists in simulators and demonstration rigs, etc.). A clear example of all these constraints may be found in the utilization of the Fluid Physics Module (Ref. 8).

4.1 Spacelab 1 experiments

For the first flight we are preparing two series of trials. In the first, a low viscosity liquid will be made to form a cylindrical zone 100 mm long, 40 mm ϕ , stand some controlled disturbances, and break, overpassing the stability limit. The second run is similar, but with a high viscosity liquid, larger dimensions (125 mm long, 60 mm ϕ) and a new breakage mode. The major steps are:

4.1.1 Filling. The disks are approached and the gap fed with liquid from a reservoir through a central hole in one of them. Disk separation is varied while filling, in order to maintain a cylindrical shape as far as possible.

4.1.2 Vibration. One of the disks is made to have small forced oscillations (up to .5 mm) at about 1 cycle per second.

4.1.3 Rotation. One of the disks is spun-up from 0 to 10 rpm. After a while, the second one is brought to counterrotation and then to isorotation.

4.1.4 Disalignment. The zone being in solid body rotation, one of the disks is laterally displaced (up to 2 mm).

4.1.5 Breakage. The disruption of the liquid bridge is intentionally pursued. In the first run this is accomplished by adding liquid and stretching the zone as to maintain the cylindrical shape, and in the second, by just withdrawing liquid at constant disk-separation. Both paths can be followed in Fig. 9, which, at the same time, summarizes the hydrostatic behavior of floating liquid zones.

4.1.6 Reattachment. The two spherical caps formed after breakage, are brought to contact, then sucking the liquid back to the reservoir.

In the whole, the experiments last about two hours, demands permanent attendance from an operator, and will supply more than 3000 black & white pictures of the liquid zone. We have already started to care about this huge amount of data: Figure 10 gives a broad view of the analysis foreseen (because of its complexity and tremendous effort required, a cooperative post-flight work among the FPM users would greatly reduce costs and delay time).

5. RESEARCH PROGRAM FOR FUTURE FLIGHTS

An outgrowth of the experimentation scheduled for Spacelab 1 is considered vital for the right fulfilment of the research aims. The following experiments take full advantage of the FPM capabilities, or require minor improvements in the facility.

First, we will go on with the analysis of equilibrium shapes and their stability, exploring new areas as the catenoidal breakage or the non-axisymmetric configurations.

Second, we would centre in the boundary layers, corner region, free surface layer and free shear layer.

And third, we would try to deal with the effects of jets (perhaps the most obvious example of jet flow occurs when filling the floating zone).

ACKNOWLEDGEMENT

Founding for these investigations is provided by the Spanish National Commission for Space Research.

REFERENCES

1. Carruthers J R et al 1975, Studies of rotating liquid floating zones on Skylab IV, *AIAA Paper* No. 75-692.
2. Benz K W 1974, Single crystals of electronic materials grown in space environment, *ESRO SP* 101, 163-170.
3. Paddy J F 1976, Capillary forces and stability in zero-gravity environments, *ESA SP* 114, 447-454.
4. Haynes J M 1976, Capillary instabilities in 0g and 1g, *ESA SP* 114, 467-472.
5. Napolitano L G 1978, Microgravitational fluid dynamics, *2nd Levich Conference*, Washington.
6. Kármán Th v 1921, Über laminare und turbulente reibung, *Z angew Math Mech* I, 233-251.
7. Benton E R & Clark A 1974, Spin-up, *Ann Rev Fluid Mech* 6, 257-280.
8. Martínez I 1979, Fluid Physics Module utilization brochure, *ESA*.

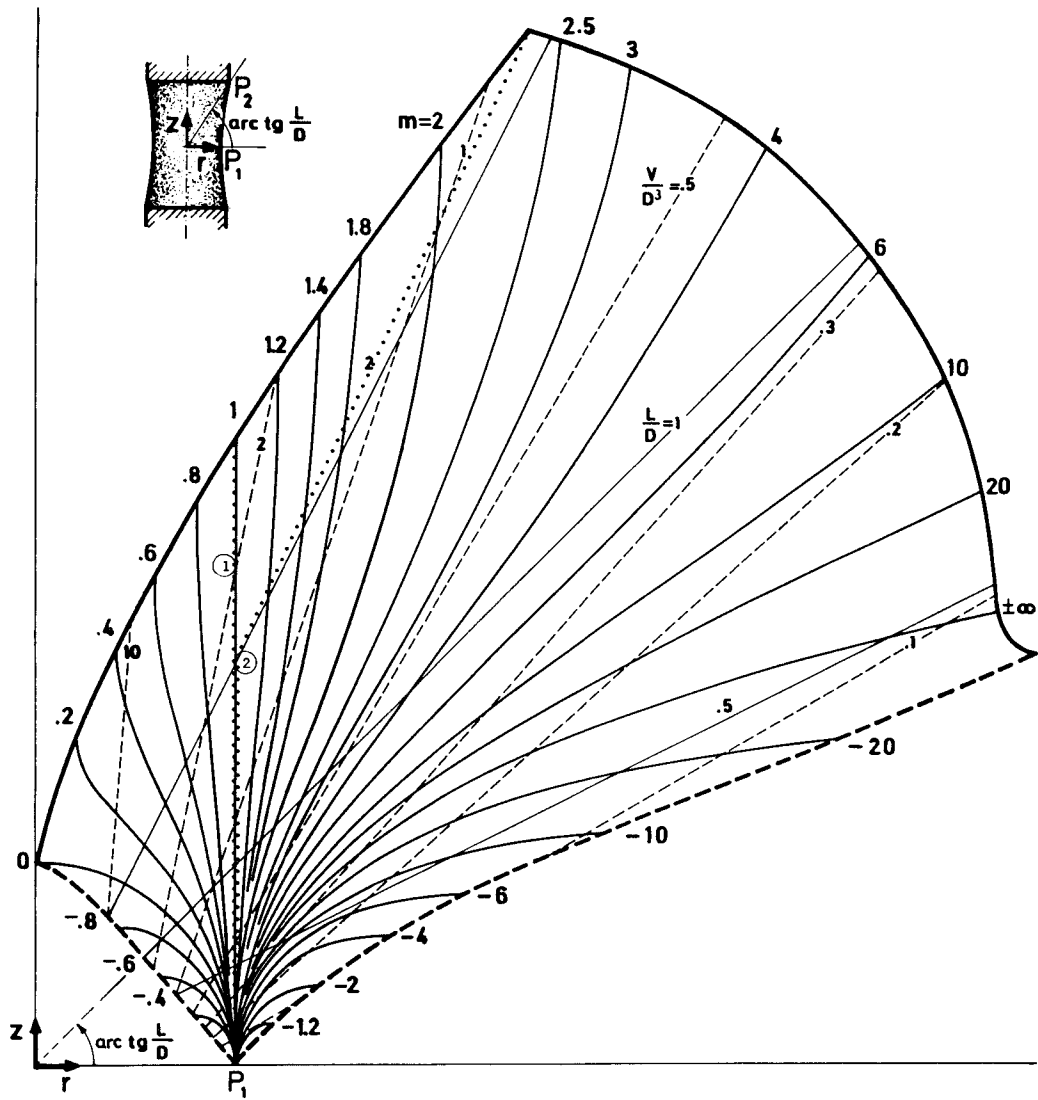


Figure 9. Summary diagram of the hydrostatic of a floating liquid zone held between two equal disks of diameter D a distance L apart. Three families of curves are drawn: the possible equilibrium shapes ($m=\text{constant}$), the loci of equal slenderness ($L/D=\text{constant}$) and the loci of equal volume ($V/D^3=\text{constant}$). The problem is solved finding in the graph the successive points P_2 (see insert) corresponding to the desired state or evolution. (m is an intrinsic geometric parameter characterizing the type of the free surface).
 evolution and working point for run ① and run ② for Spacelab 1.

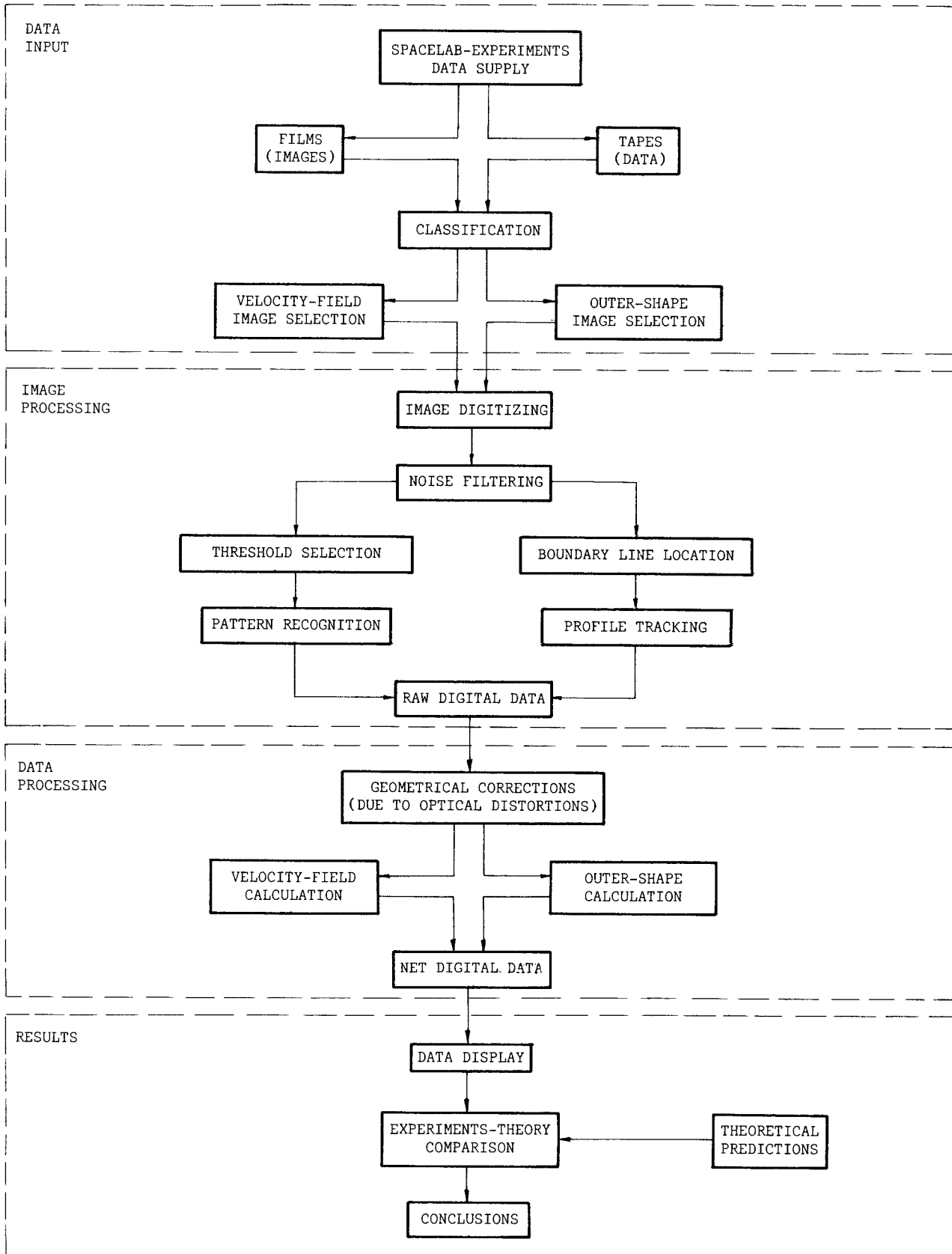


Figure 10. General block-diagram of the post-flight data analysis foreseen for the appropriate completion of this research.